YIELD-STRESS ANALYSIS OF ELASTO-VISCO-PLASTIC MATERIALS IN CROSS-SLOT GEOMETRY

A. Kordalis[1], S. Varchanis[1], I. Tsamopoulos[1]*

[1]Department of Chemical Engineering, University of Patras, Patras, Greece

(*tsamo@chemeng.upatras.gr)

ABSTRACT

While much attention has been paid in the rheological response of elasto-visco-plastic materials in shear flows, surprisingly few studies have focused on pure extensional flows of such materials. This fact is probably associated with the practical difficulties related with the generation of a purely extensional flow field. In addition, recent experiments by Zhang et al.[1] have revealed noticeable differences with respect to the extensional behaviour of complex yield-stress materials (i.e. the ratio of the extension yield-stress to the shear yield-stress is larger, by a factor of 1.5, than expected from the standard theory). Such findings indicate the importance of the investigation of the yield-stress materials in elongational flows. We propose the standard cross-slot device to measure the extensional properties of complex yield-stress fluids. More specifically, we fit the Saramito/Herschel-Bulkley[2] model to a 0.08% Carbopol solution and carry out simulations of elasto-visco-plastic flows in the standard cross-slot geometry. Performing a wide-range parametric analysis on the dynamics of this stagnation flow, we show that due to the low elasticity of these materials, it is possible to obtain a steady state vorticity-free flow around the stagnation point even for high extension rates. The impact of the interplay of plasticity and elasticity on the nonlinear dynamics of the cross-slot flow are examined in detail.

INTRODUCTION

In everyday life, we come across numerous materials that flow above an applied stress, otherwise they behave like solids. Their response when motion is induced is determined based on the imposed flow conditions. This kind of materials are described as yield stress materials. For example, spreading mayonnaise on a slice of bread reveals the flowing nature of the material. On the other hand, the corrugations created on the free surface of mayonnaise after agitating the content of a jar, remain in place and won't flatten under the constant stress generated by gravity. This reveals the solid nature of this material. The same material displays two radically different behaviours in two slightly different situations. In the first case the applied stress magnitude is large enough to make the mayonnaise flow, while in the second case the magnitude of stress is inadequate to make the system flow. Somewhere between, there is a value of stress in which the transition from solid to fluid occurs. This threshold is called yield stress. The proper spotting of the material areas where fluidization takes place is a matter of great importance. Thus, a robust criterion is needed for tracking the yield surface. The most widely accepted criterion is that proposed by Von Mises as its predictions are very accurate and have been evaluated experimentally[3].

A yield stress response is observed in a vast variety of materials like pastes, powders, suspensions, gels and emulsions[4]. Despite the gaping differences in the structure of those media, the phenomenological yield stress mechanism under which they behave is surprisingly similar[5]. The significance of the identification of the rheological response of such materials lies in the plethora of applications that they appear. Yield stress materials play a key role to many processes involving industrial, research and financial interest. Some examples are the processing of pulp suspensions of paper making[6], preparation of concrete in construction[6] and extraction of crude oil[7]. As studied by Dimitriou and Mckinley[7], crude oil demonstrates intricacies during extraction. Specifically, the pressure drop (therefore energy consumption as well as a priori dimensioning of equipment, i.e. pumps) required to restart a gelled pipeline is proportionate to the yield stress of the material. Consequently, a proper characterization of the rheological response of waxy crude oil is necessary in order to design accurately the drilling and extraction process. Up to this day, this characterization

is based only on shear rheology neglecting extensional contributions. However, Zhang et al.[1] illustrated experimentally that the extensional response of yield stress materials may be quite different than their shear response, highlighting that the standard viscoplastic theory (Bingham model) cannot predict such differences.

The main objective of this study is to examine the response of yield stress materials when subjected to extensional deformations. The material that we choose to focus on is a well-characterized Carbopol solution[8]. The main reason behind the thorough research on this material is its "ideal" or non-thixotropic behaviour that provides a better understanding of its elastic and plastic properties. We choose the standard cross slot geometry in order to generate a planar, two-dimensional extensional flow field. The constitutive model that describes the rheology of Carbopol in this study is the Saramito/Herschel-Bulkley, i.e. SRM/HB[2]. According to Fraggedakis et al.[9], who performed recently a comparison among the predictions of various elasto-visco-plastic (EVP) constitutive models, the SRM/HB model can capture the rheological response of EVP materials more accurately, when compared to other EVP models. At the same time it maintains a rather simple form, hence its adoption is favoured over other existing EVP models.

PROBLEM FORMULATION

An incompressible elasto-visco-plastic material is found at rest inside the microscale planar cross slot geometry (Fig. 1). Symbols bearing the superscript * correspond to dimensional quantities, otherwise they correspond to dimensionless quantities. When subjected to motion under levels of stress lower than the yield stress τ_y^* , the material behaves as a Neo-Hookean solid with elastic modulus G^*. Otherwise it flows as a viscoelastic fluid [2] with an apparent relaxation time $\lambda^* = (k^*/G^*)^{1/n}$ where k^* is the consistency parameter and n the exponent of Herschel-Bulkley model. As shown in Fig. 1, the width and length of each channel of the cross slot are equal to H^* and $L^* = 10H^*$, respectively, following the design by Cruz et al.[10]. There are two inflows, on the top and bottom arm, as well as two outflows at the left and right arm. Also, to avoid stress singularities in the cross-slot flow, we use rounded corners, with a radius equal to 5% of the channel width. The effect of gravity is neglected as the gravitational field is perpendicular to the planar flow. All lengths are scaled with the width of the channel H^*, whilst the velocity field is scaled with the mean velocity at the inflow U^*. Stresses and pressure are scaled with G^*. Therefore the dimensionless numbers that arise are the Reynolds number, $Re = \rho^* U^{*2}/G^*$, the Weissenberg number, $Wi = \lambda^* U^*/H^* = (k^*/G^*)^{1/n} U^*/H^*$, the yield strain $\varepsilon_y = \tau_y^*/G^*$ and the Bingham number $Bn = \varepsilon_y/Wi$. Note that the density of the material is denoted as ρ^*. The Bingham number is expressed as a function of the *Wi* and the yield strain (Bn = εy/Wi). Note that the Bingham number is inversely proportional to the Weissenberg number. Thus, when the Bingham number is large, the material behaves like an elastic solid. On the contrary, when the Bingham number is small the material behaves like a viscoelastic liquid.

Initially, the material does not carry any stresses in its bulk. At a certain time instant, the flow rate is suddenly elevated from zero to a prescribed value at the inflows of the geometry and the EVP flow starts to evolve in the cross-slot geometry.
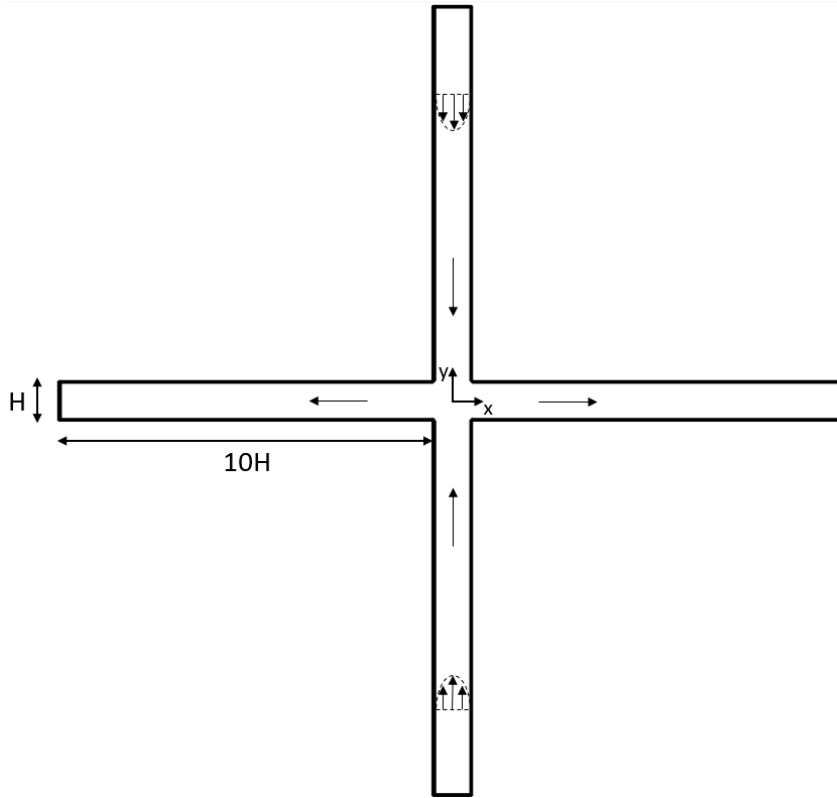
Figure 1. *In scale schematic representation of the planar cross slot geometry containing a yield stress fluid under flow.*

GOVERNING EQUATIONS

In all simulations, we assume incompressible, isothermal and creeping flow ($Re = 0$). These features are expressed in a non-dimensional form by the mass balance and the momentum balance as follows:

$$\underline{\nabla} \cdot \underline{u} = 0 \tag{1}$$
$$\underline{\nabla} \cdot \underline{\underline{\sigma}} = \underline{0} \tag{2}$$

where $\underline{u}$ is the velocity vector and $\underline{\underline{\sigma}}$ represents the total stress tensor.

The total stress tensor is split in an isotropic part containing the thermodynamic pressure P and a part that includes the extra stress tensor $\underline{\underline{\tau}}$ contribution. The latter is due to the elasto-visco-plastic nature of the material. Hence, the total stress tensor is given in terms of conformation tensor $\underline{\underline{C}}$ where $\underline{\underline{\tau}} = \underline{\underline{C}} - \underline{\underline{I}}$ as:

$$\underline{\underline{\sigma}} = -P\underline{\underline{I}} + \underline{\underline{C}} - \underline{\underline{I}} \tag{3}$$

The non-Newtonian elasto-visco-plastic stesses of the fluid are expressed via the Saramito constitutive model which has the following tensorial form:

$$\overset{\nabla}{\underline{\underline{C}}} + \frac{f\left(\underline{\underline{C}}\right)}{Wi}\left(\underline{\underline{C}} - \underline{\underline{I}}\right) = \underline{0} \tag{4}$$

Where the first term of the above equation is the Upper Convected Maxwell derivative of the conformation tensor and $f\left(\underline{\underline{C}}\right)$ is the function that governs the transition of the material from an unyielded to a yielded state and vice-versa. According to the SRM/HB implementation[2] we have:

$$f\left(\underline{\underline{C}}\right) = \max\left[0, \frac{|\underline{\underline{\tau}}_D| - \varepsilon_y}{|\underline{\underline{\tau}}_D|^n}\right]^{1/n} \tag{5}$$

Where the second invariant of the deviatoric stress tensor $\underline{\underline{\tau}}_D = \underline{\underline{\tau}} - \frac{tr\left(\underline{\underline{\tau}}\right)}{3}\underline{\underline{I}}$ is given as:

$$\left|\underline{\underline{\tau}}_D\right| = \sqrt{\frac{\underline{\underline{\tau}}_D : \underline{\underline{\tau}}_D}{2}} \tag{6}$$

The governing equations are solved numerically using the newly proposed stabilized finite element method by Varchanis et al.[11], that features equal order interpolation of all variables (velocities/pressure/stresses) and makes use of the log-conformation representation of the constitutive equation. The domain is discretized in triangular elements using the quasi-elliptic mesh generator proposed by Dimakopoulos and Tsamopoulos[12]. Finally, fully implicit transient simulations are performed in order to investigate and understand the nonlinear dynamics of this stagnation point flow.

FLUID RHEOLOGY

The data used to estimate the values of the material parameters of the model are obtained by the experimental observations of Putz et al.[8]. The model contains 4 parameters to be fitted. These are G^*, τ_Y^*, k^* and n. G^* is extracted from LAOStress experiments, while the remaining parameters are estimated by fitting the predictions of the model to the experimental flow curve (steady shear stress vs shear rate). The values of the material parameters are presented in Table 1.

Table 1. *Values of the parameters of SRM/HB model obtained by fitting the SRM/HB model to the experimental data of Putz et al. [add reference].*

G^* (Pa)	τ_Y^*,(Pa)	k^* (Pa s^n)	n
62.5	1.62	4.84	0.33

For the base case, the yield strain ε_y equal to 2.67 10^{-2}.

RESULTS AND DISCUSSION
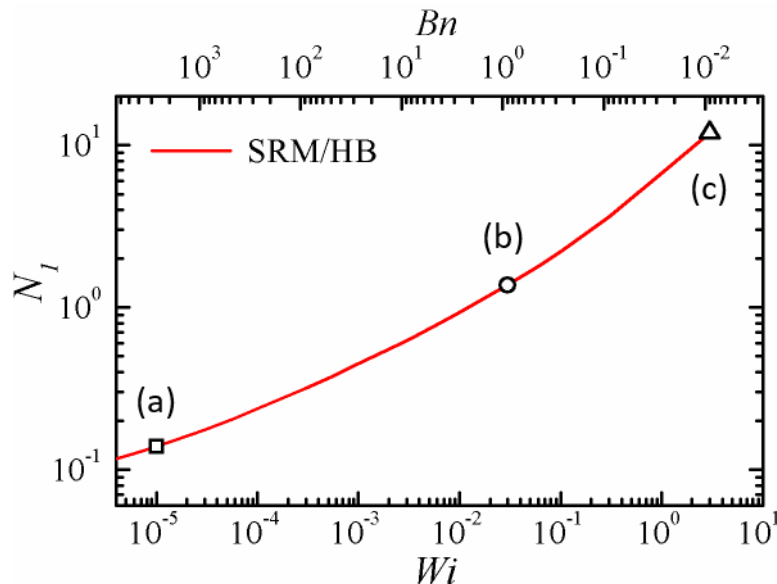
Figure 2. *N₁ vs Wi at the stagnation point of the cross-slot geometry. Point (a) corresponds to Wi=10^{-5}, (b) to Wi=0.03 and (c) to Wi=3.*

Fig. 2 presents the predicted steady first normal stress difference ($\tau_{xx}-\tau_{yy}$), which is denoted as N_1, as a function of the *Wi* number. At the upper axis of the figure, we present the respective *Bn* number. The distinct points (a), (b) and (c) in Fig. 2 are chosen for depicting close-ups of the CSER device at certain *Wi* numbers. At the right part of each close-up in Fig. 3 we present the streamlines of the flow, superimposed on the yield surfaces. In the regions of the geometry that are red, the material is in a yielded state, while in the regions of the geometry that are blue, the material is in

an unyielded state. At the left part of the close-ups we show the contours of N_1. Starting from very low values of the flow rate, we can observe that N_1 forms a plateau. This plateau resembles the plateau at simple shear flow experiments, defining a yield normal stress. At higher flow rates, N_1 rises just like in viscoelastic fluids. Note that we find steady states with symmetric flow fields for all flow rates examined in this case. Now, examining the close-ups of the CSER for low flow rates, we can observe that unyielded regions exist before and after the stagnation point. With increasing flow rate, the unyielded regions vanish and the flow enters a viscoelastic regime. The material particles become more and more stretched in the x-direction and the streamlines feature a bending shape close to the stagnation point, something that is a clear sign of viscoelasticity. Similar streamlines and N_1 profiles have been observed in the viscoelastic fluid experiments [13].
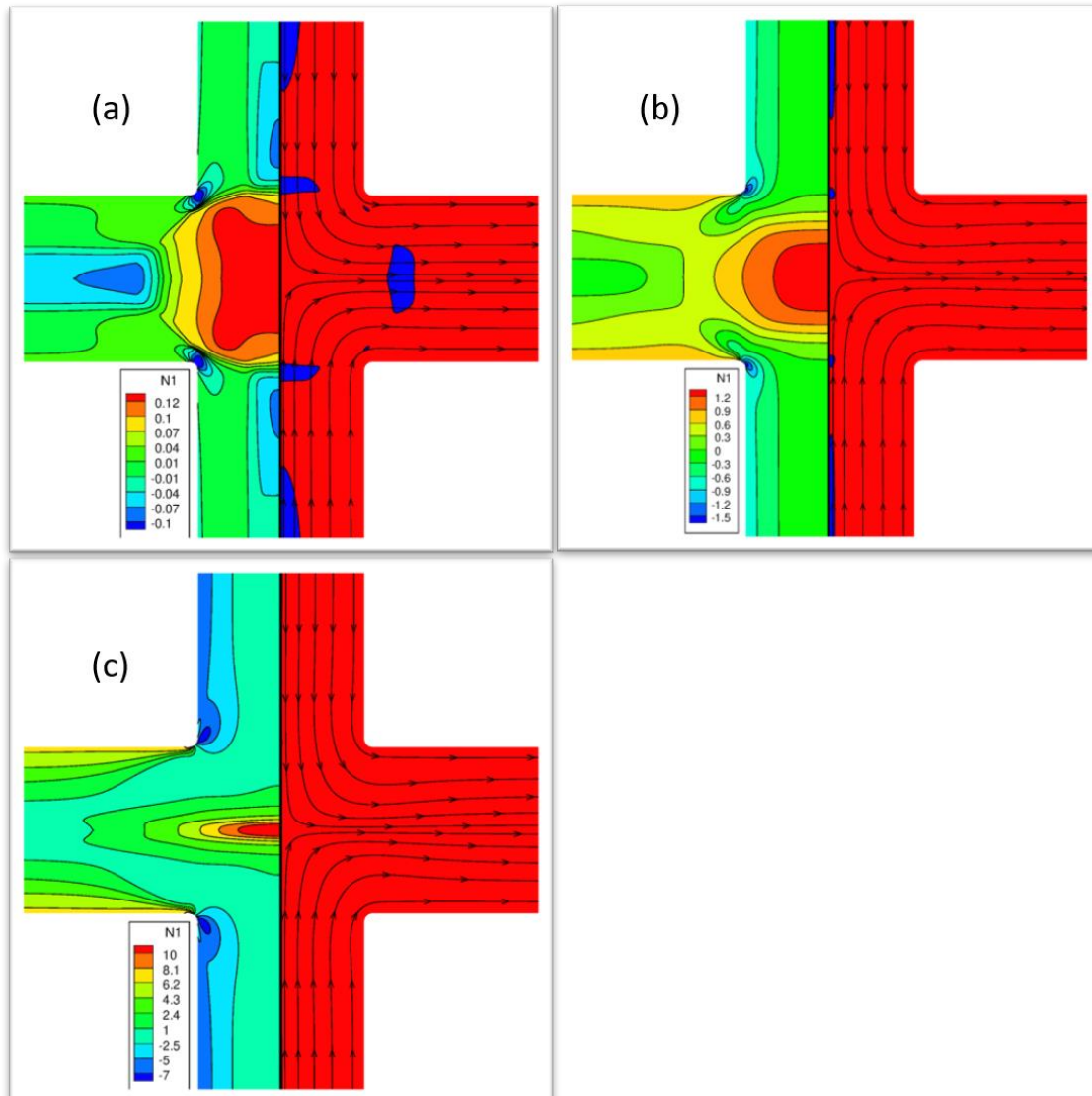
Figure 3. Contours of N_1 at the left and streamlines superimposed with yielded/unyielded areas at the right for cases (a) Wi=10^{-5}, (b) Wi=0.03 and (c) Wi=3. highlighted in Figure 2.

CONCLUSIONS

We have examined the flow of elasto-visco-plastic materials in the standard cross slot microfluidic device. This device can provide valuable information with respect to the normal stresses that develop in yield-stress materials. At low flow rates, elastoplastic effects and the normal yield stress can be evaluated. At high flow rates, the viscoelastic effects of yield stress materials can be evaluated. Finally, due to the low elasticity of yield stress materials, a symmetric steady flow field can be established for a wide range of imposed flow rates.

REFERENCES

[1]   X. Zhang, O. Fadoul, E. Lorenceau, P.Coussot. Phys. Rev. Lett., 120(4), (2018), 048001.

[2]   P. Saramito. J. Non-Newtonian Fluid Mech., 158(1-3), (2009), 154-161.

[3]   G. Ovarlez, Q. Barral and P. Coussot. Nat. Mater., 9, (2010), 115-119.

[4]   D. Weaire, J. D. Barry S. Hutzler. J. Phys.: Condens. Matter, 22, (2010), 193101.

[5]   P. Coussot, J. S. Raynaud, F. Bertrand, P. Moucheront, J. P. Guilbaud, H. T. Huynh, S. Jarny, D. Lesueur. Phys. Rev. Lett., 88(21), (2002), 218301.

[6]   N. J. Balmforth, I. A. Frigaard, G. Ovarlez. Annu. Rev. Fluid Mech., 46, (2014), 121-146.

[7]   C. J. Dimitriou G. H. McKinley. Soft Matter, 10, (2014), 6619.

[8]   A. M. V. Putz, T. I. Burghelea, I. A. Frigaard, D. M. Martinez. Physics of Fluids, 20, (2008), 033102.

[9]   D. Fraggedakis, Y. Dimakopoulos, J. Tsamopoulos. J. Non-Newtonian Fluid Mech., 236, (2016), 104–122.

[10] F.A. Cruz, R.J. Poole, A.M. Afonso, F.T. Pinho, P.J. Oliveira, M.A. Alves. J. Non-Newtonian Fluid Mech., 214, (2014), 57–68.

[11] S. Varchanis, A. Syrakos, Y. Dimakopoulos, J. Tsamopoulos. J. Non-Newtonian Fluid Mech., 267, (2019), 78-97.

[12] Y. Dimakopoulos, J. Tsamopoulos. J. Comput. Phys., 192, (2003), 494–522.

[13] S. J. Haward, G. H. McKinley, A. Q. Shen. Scientific Reports, 6, (2016), 33029.